Pergamon

Scripta Materialia, Vol. 38, No. 3, pp. 363–368, 1998
Elsevier Science Ltd

1359-6462/98 $19.00 + .00

PII S1359-6462(97)00502-2

THE DEFORMATION TEXTURE IN A $Ti_{49}Ni_{51}$ ALLOY

T.S. Chou[1], S.K. Wu[2] and H.C. Lin[3]

[1]Steel and Aluminum R&D Department, China Steel Corporation, Kaohsiung, Taiwan 812, R.O.C.
[2]Institute of Materials Science and Engineering, National Taiwan University, Taipei, Taiwan 106, R.O.C.
[3]Dept. of Materials Science, Feng Chia University, Taichung, Taiwan 400, R.O.C.

(Received April 4, 1997)
(Accepted October 27, 1997)

Introduction

Nickel-Titanium intermetallic compounds with good shape memory effect have long time been applied in many uses [1]. During the past decade, a great deal of research has been done documenting on the investigation of phase transformation behaviour using internal friction measurement, electrical resistivity, differential scanning calorimeters, and the TEM observations [2–5]. However, little research has been done on crystallographic textures [6,7]. To open up more applications on these distinctive alloys, a refined understanding of the crystallogaphic texture is necessary. In this work, the binary $Ti_{49}Ni_{51}$ alloy was deformed at different temperatures to investigate the corresponding crystallographic textures. This study on crystallographic textures was pursued using X-ray pole figure measurement, in which the precise analysis using ODFs (Orientation Distribution Functions) was applied.

Experimental Procedure

The $Ti_{49}Ni_{51}$ alloy was applied in this study and was prepared by the conventional vacuum arc remelting technique. Titanium (purity, 99.9%) and nickel (purity, 99.9%) for the experimental alloys were melted and remelted at least four times in an argon atmosphere. The mass loss during the melting was negligibly small. The as-melted buttons were homogenized at 1050 °C for 72 hours and quenched in water, then subsequently reheated to 1000 °C for hot-rolling into plates. The hot-rolled plates with 1 mm thickness were again homogenized under the same conditions. The deformation experiments were carried out under the change of temperatures and reduction ratios. The details of the working conditions were shown in Table 1.

Specimens with the size 150 mm × 250 mm were carefully cut from the plates with a low-speed diamond saw for X-ray pole figure measurements. The pole figure measurements were conducted using the *Simens* 500 X-ray diffraction method. Before the measurement of pole figures, the diffraction method was used to determine the precise 2θ angle range for the determination of measured pole planes. The pole figures using the X-ray back- reflection technique after Schulz using Mo-radiation were acquired [8]. The orientation distribution functions (ODFs), including odd terms for ghost correction, were then calculated up to an order of $l_{max} = 20$ by the series expansion method [9], and the ODFs were most concisely represented and compared by fibre texture analysis [10].

TABLE 1
The Deformation Conditions of $Ti_{49}N_{51}$ Alloy

Sample I.D.	Deformation Temperature, °C	Reduction Ratio, %	Deformed Structure
A-1	−196	15	B19′ martensite
A-2	25	30	B2 parent phase

Results and Discussion

$Ti_{49}Ni_{51}$ alloy has a martensitic transformation temperature of around −90 °C and a cubic B2 structure at room temperature [11]. To investigate the deformation effect on the crystallographic texture, the deformation processes were conducted at the liquid nitrogen temperature and room temperature, respectively. The measurement of pole figures data were carried out at the B2 temperature. The low temperature deformed sample can thus provide a study on the reversed transformation texture from the deformed martensite phase to the parent B2 phase. The room temperature deformed sample can be used to further investigate the deformation effect on the B2 structure.

Before the pole figure measurement, the X-ray diffraction method was applied to identify the 2θ angle to determine the required pole planes for further texture measurement. Figure 1 shows the X-ray intensity as a function of 2θ value for A-1 and A-2 samples. It was found that the liquid nitrogen temperature deformed sample (A-1) has an X-ray diffraction spectrum similar to the one deformed at room temperature (A-2), although the former sample shows diffraction peaks somewhat intensified. However, the differences between these two are insignificant. From the X-ray spectra, the most pronounced peaks in both samples are (110) and (112). The stronger (200) peak normally found in the conventional low carbon steel sheets is not the case in $Ti_{49}Ni_{51}$ alloy.

Therefore, the ongoing pole figure measurement was carried out using the two pole planes (110) and (112), and the ODFs were calculated based on the measured pole figures. To verify the reliability of the ODFs results the calculated pole figures were compared with the measured ones in Figures 2. A good agreement between the measured and calculated results was obtained. Therefore, the ODFs calculations are reasonable.

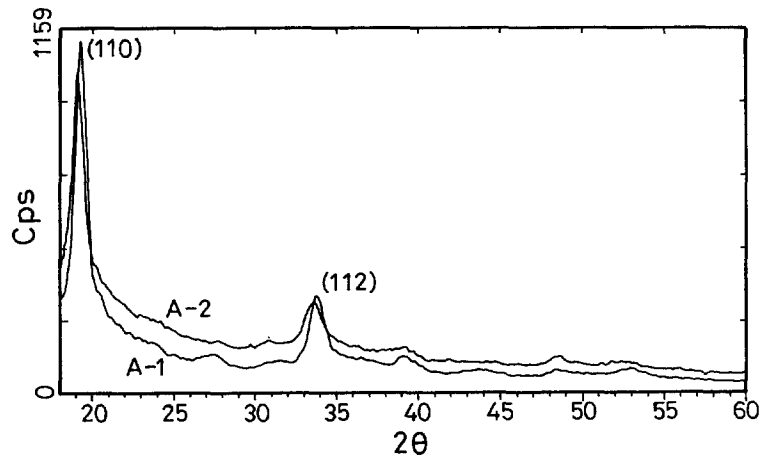

Figure 1. The X-ray diffraction (XRD) spectra of the $Ti_{49}Ni_{51}$ alloy as deformed at (a) liquid nitrogen temperature (A-1), and (b) room temperature(A-2). The XRD measurement was conducted at room temperature.

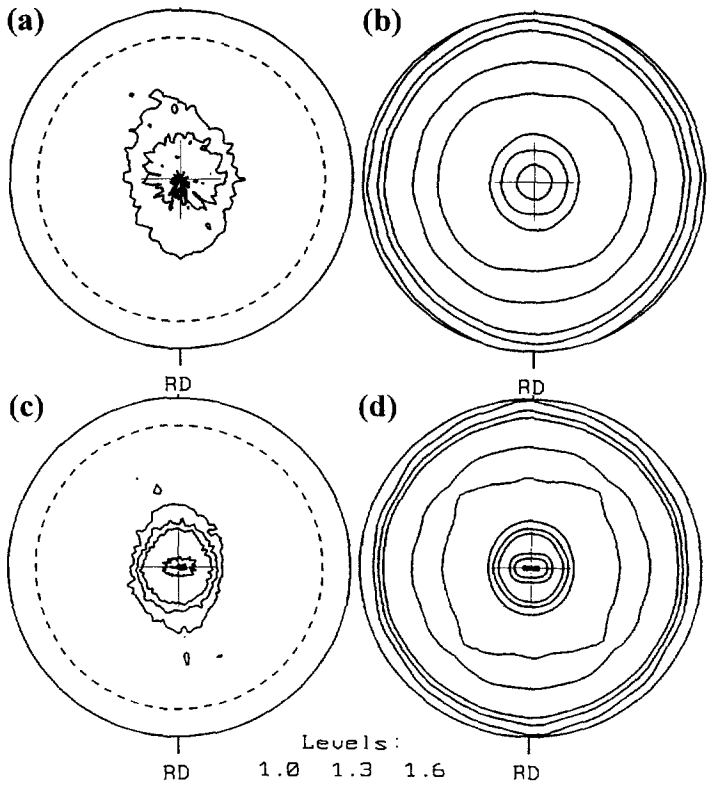

Figure 2. The comparison of measured pole figures with the calculated results. (a) measured (112) pole figure of A-1 sample, (b) calculated (112) pole figure of A-1 sample, (c) measured (112) pole figure of A-2 sample, (d) calculated (112) pole figure of A-2 sample.

Figure 3 and Figure 4 illustrate the ODFs results. It is found that there are only the ND-type fibres (crystalline planes in parallel with the normal direction in sample's geometric coordination) in the deformed $Ti_{49}Ni_{51}$ alloy. Other geometric direction type fibres, such as α-fibre (which has $\langle 110\rangle$//rolling direction) and η-fibre (which has $\langle 001\rangle$//RD) normally found in the deformed steel sheets [12], were never found in the deformed $Ti_{49}Ni_{51}$ alloy. The ND-type fibres in the deformed $Ti_{49}Ni_{51}$ samples encompassed the components {551}, {557} and {332} in both of B2 phase and martensite phase deformed samples. The {557} ND fiber at the Phi2 = 45°, Phi = 45°, and Phil from 0° to 90° (Bunge notation), which can be rotated 10° along $\langle 110\rangle$axis from the {111} ND fibre towards the {112} ND fibre. On the other hand, the {551} ND fibre located at the ODFs cuts Phi2 = 45°, Phi = 81.2° and Phil from 0° to 90° is close to the {110} ND fibre. The {332} ND fibre located at the ODFs cuts Phi2 = 45°, Phi = 62.5 ° and Phi1 from 0° to 90°. Due to the crystallographic symmetry, the same ND fibres can be found at the different ODFs cut, for example {551} ND fibre at Phi2 = 80°, Phi = 45°, and Phil from 0° to 90°. Compared with these two ODFs results, the B2 phase deformed sample has a significantly sharpened fibre texture than the low temperature deformed sample.

Plastic deformation in metal occurs due to dislocations gliding, slipping or deformation twinning under some particular crystallographic planes and directions. However, the amount of the slipping system is highly depended on the alloy composition and deformation condition of metal. On the other hand, the twinning systems are normally found to be {111}$\langle 112\rangle$ type in FCC structure, or

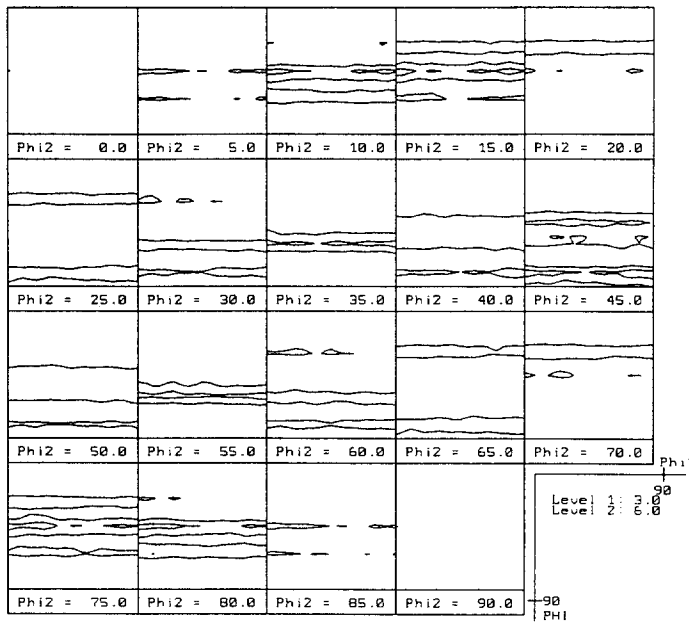

Figure 3. The ODFs of $Ti_{49}N_{i51}$ alloy as deformed at liquid nitrogen temperature.

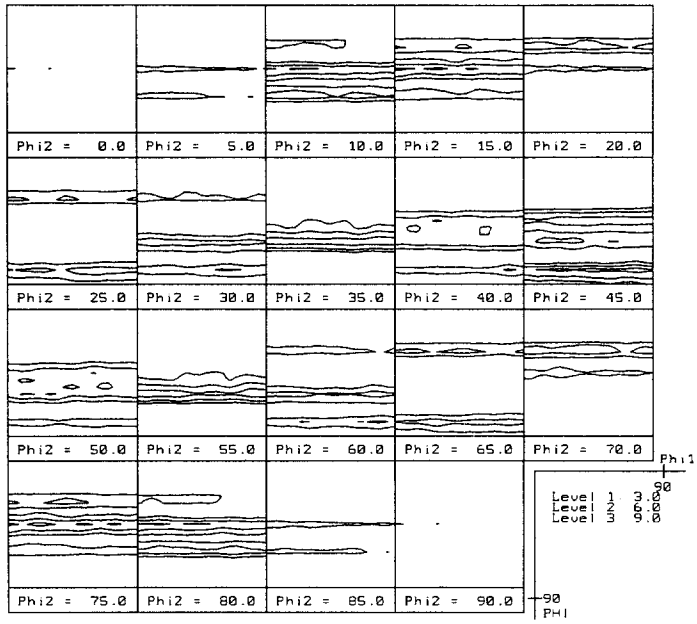

Figure 4. The ODFs of $Ti_{49}N_{i51}$ alloy as deformed at room temperature.

{112}⟨111⟩type in BCC structure [13]. Although mechanical twinning might change the twinning direction, most of the plastic deformation is dominated by the dislocation slipping [14]. During deformation, crystallites rotate along the stress axis, which leads to the energy stable end direction. For example, the preferred slip direction will rotate toward the deformation direction during the tensile test. In addition, the easier slip planes in sheet metals rotate until their normal direction is parallel with the compression direction. The deformation texture in metals is thus affected by the crystallographic structure, deformation type, chemical composition, deformation temperature and the initial texture.

Generally, the deformation (rolling) texture between surface and central region can be very different due to the shearing effect caused by the friction of roller and sheet surface. The variation of shear deformation to affect the surface texture can normally be controlled by the factor lc/d [15], in which lc is the contact length between roller and sheet, and d the gap of the rollers. A significant shear deformation effect on the surface texture is found under a small lc/d condition. When lc/d is larger than 1, the shear effect is reduced dramatically similar to the plain strain compression.

The surface texture of strong intensity ζ-fibre with the components between (011)[100] and (011)[211] has been found in the hot-deformed Al-killed steels to clearly indicate shear-texture type [16]. A similar result is found in the deformed high strength steels. However, the ζ-fibre in both conditions is approximately diffuse and other fibres are also involved although the relative intensity is very low [17].

In case of deformed $Ti_{49}Ni_{51}$ alloy, the finding of ζ-fibre may more easily be confused with the surface shear texture because the pole figure measurement was carried out on the sample surface. However, a refined consideration confirms that the ζ-fibre is coming from the crystallographic characteristic of this alloy not simply from the shearing effect during the deformation process since the critical lc/d is larger than 1, therefore, the shear effect is reduced dramatically similar to the plain strain compression. Moreover, the other ND fibres are also found in the deformed $Ti_{49}Ni_{51}$ alloy, and the ζ-fibre in the deformed $Ti_{49}Ni_{51}$ alloy has a much more sharpened feature than the diffused surface texture observed in normally deformed steels.

Basically, the deformed martensite phase can transfer into the B2 structure in terms of twinning upon heating up to room temperature for the $Ti_{49}Ni_{51}$ alloy, which results in a crystallographic texture akin to the sample deformed at parent phase. However, the room temperature deformed sample could have the further intensified deformation texture. The enhancement of (551) ND fibre implied that this crystallographic plane should have the higher Schmid factor thus provide the ease for slip or accommodation of the material flow during deformation or phase transformation. Therefore, the (551) plane is suspected to be one of the habit planes for slip or twinning during deformation. In heating, the liquid nitrogen temperature deformed texture can be completely inhibited by the transformation of martensite to the B2 phase.

The phase transformation was carried under conditions of twinning. Therefore, a difference of textures in the samples deformed at different phases can be regarded as the effect of the deformation ratio on the development of crystallographic texture. The finding of the unique ND-type fibres in the deformed $Ti_{49}Ni_{51}$ alloy implied that the materials flow of this alloy was carried out in terms of twinning rather than the gliding in conventional carbon steel during the course of deformation, which can explain the superelastic characteristic of the many thermal-elastic type shape memory alloys.

Instead of the many other fibres found in the deformed conventional low carbon steel sheets, such as α and η, there are always one kind of ND fibre texture in the deformed TiNi alloy. The finding of unique ND fibres in the deformed TiNi alloy is consistent with the martensitic transformation mechanism in this alloy. The twinning is parallel to the shearing direction movement of the twinning boundaries. The improved superelasitic characteristic normally found in the deformed TiNi shape memory alloys [18] is suspected due to the existence of those unique ND-fibres.

Summary

Crystallographic textures of binary $Ti_{49}Ni_{51}$ alloy have been investigated using X-ray back-reflection method. The deformed $Ti_{49}Ni_{51}$ has a unique ND-type fibres, encompassing {551}, {557}and {332}, irrespective of the deformation temperature. The finding of ND-fibres confirmed that the accommodations of materials flow is conducted in terms of twinning along the shear direction during deformation. In which the ease of materials flows should be accommodated along the stress direction. Moreover, the deformation texture at low temperature martensitic phase can be entirely inhibited to the B2 phase after the reversed transformation.

Acknowledgement

The authors are pleased to acknowledge the financial support of this research by the National Science Council (NSC), Republic of China, under Grant NSC84-2216-E002-027.

References

1. T. W. During, K. N. Melton, D. Stöckel, and C. M. Wayman, in Engineering Aspects of Shape Memory Alloys, Butterworth-Heinemam Press, London (1990).
2. R. R. Hashiguti and K. Iwasaki, J. Applied Physics. 39, 2182 (1981).
3. M. B. Salamon, M. Meichel, C. M. Wayman, C. M. Hwang, and S. M. Shapiro, in Modulated Structures, ed. J. M. Cowly, J. B. Cohen, M. B. Salamon, and B. J. Bunsch, A.I.P. Conf. Proc. No. 53, New York, American Institute of Physics, 223 (1979).
4. C. M. Hwang, M. B. Salamon, M. Meichel, and C. M. Wayman, Phil Mag. A. 47, 9 (1983).
5. C. M. Hwang, M. B. Salamon, M. Meichel, and C. M. Wayman, Phil. Mag. A. 47, 31–62.
6. J. H. Mulder, P. E. Thoma, and J. Beyer, Z. Metallk. 84, 501 (1993).
7. H. Inoue, N. Miwa, and K. Inakazu, Acta Mat. 44, 4825 (1996).
8. L. G. Schulz, J. Applied Physics. 20, 1030 (1949).
9. H. J. Bunge, in Texture Analysis in Materials Science, Butterworths, London (1982).
10. U. v. Schippenbach, F. Emran, and K. Lücke, Acta Metall. 34, 1289 (1986).
11. H. C. Lin, PhD Thesis, National Taiwan Univ (1992).
12. W. Bleck, R. Grobterlinden, U. Lotter, and C. Reip, Steel Research. 12, 580 (1991).
13. D. Hull, in Introduction to Dislocations, pp. 122–147, Pergamon Press (1975).
14. H. Hu, Texture. 1, 233 (1974).
15. J. Hansen and H. Mecking, in ICOTOM-4, Metal Society, pp. 34–47 (1975).
16. W. Bleck, R. Grobterlinden, U. Lotter, and C-P Reip, Steel Research. 62, 580 (1992).
17. C. Därmann and B. Engl, Steel Research. 62, 576 (1992).
18. H. C. Lin and S. K. Wu, Acta Met. Mat. 42, 1623 (1994).